Transient Dynamics of Coherent Waves Released from Quantum Billiards and Analogous Observation from Free-Space Propagation of Laser Modes

C. C. Chen, Y. T. Yu, Ross C. C. Chen, Y. J. Huang, K. W. Su, Y. F. Chen,* and K. F. Huang
Department of Electrophysics, National Chiao Tung University, 1001 Ta Hsueh Road, Hsinchu, Taiwan
(Received 2 October 2008; published 30 January 2009)

The transient dynamics of the eigenstates and coherent states released from a square quantum billiard is analytically and numerically investigated. It is experimentally verified that this transient dynamic can be analogously observed with the free-space propagation of the lasing modes emitted from the laterally confined, vertically emitted cavities. Furthermore, we exploit a chaotically shaped cavity to originally demonstrate the diffraction-in-time characteristics of the chaotic wave functions. It is found that the transient patterns of chaotic wave functions exhibit a striking feature of random branching behavior with the appearance of intricate interference fringes.

DOI: 10.1103/PhysRevLett.102.044101 PACS numbers: 05.45.Mt, 03.65.−w, 42.55.Px, 42.60.Jf

One of the most relevant quantum transient phenomena in matter waves is the diffraction-in-time effect for a suddenly released coherent beam, which appears to have first been introduced by Moshinsky in 1952 [1]. The hallmark feature of the diffraction-in-time effect is the temporal quantum interference patterns, by analogy with the spatial interference patterns of light diffracted by a sharp edge [2–5]. The experimental test for this effect was indeed hard to reach at the time of its first introduction. However, because of the development of an ultrafast laser [6], atom cooling, and optical trapping [7], the transient dynamics has been recently observed in a wide variety of systems including neutrons [8], ultracold atoms [9], electrons [10], and Bose-Einstein condensates [11].

Another physical connection to the diffraction-in-time effect would be the transient response to abrupt changes of the confined potential in semiconductor structures and quantum dots [12,13]. Semiconductor quantum dots, in which electronic motion is predominately ballistic in nature, have been widely used as two-dimensional (2D) quantum billiards to explore the properties of quantum chaos [14–16]. Understanding the time evolution of suddenly released quantum-billiard waves has some important applications, as it can provide the nanostructure transport properties for developing novel ultrahigh-speed semiconductor devices [12]. Moreover, it is closely related to atom laser dynamics from a tight waveguide whose boundary shape can be modified with the laser trapping beam [13,17]. Nevertheless, the investigation for the transient dynamics of 2D quantum-billiard coherent waves has not been performed as yet.

In this Letter we first theoretically investigate the diffraction-in-time effect of quantum eigenstates in square billiards. We further use the analytical result to explore the transient dynamics of the quantum coherent states that have intensities to concentrate on the classical periodic orbits. With the numerical visualization and experimental identification, we verify that the transient dynamics of coherent waves suddenly released from quantum billiards can be analogously observed with the free-space propagation of the lasing modes emitted from the laterally confined vertically emitted cavities. More importantly, we design a chaotically shaped laser cavity to experimentally demonstrate for the first time the characteristics of the diffraction in time of the chaotic billiard waves.

The 2D square billiard is one of the simplest billiards in classical mechanics [18,19]. The quantum eigenstates $\psi_{\tilde{m},\tilde{n}}(x, y)$ for the vertices are at $(\pm a/2, \pm a/2)$ and $(\pm a/2, \mp a/2)$ and are given by

$$\psi_{\tilde{m},\tilde{n}}(x, y) = (2/a)\sin[k_{\tilde{m}}(x + a/2)]\sin[k_{\tilde{n}}(y + a/2)], \quad (1)$$

where $k_n = n\pi/a$ $(n = 1, 2, 3, \ldots)$ and a is the length of the square boundary. In terms of the 2D free propagator, the free time evolution of the eigenstates $\psi_{\tilde{m},\tilde{n}}(x, y)$ suddenly released at time $t = 0$ is given by [1,2]

$$\psi_{\tilde{m},\tilde{n}}(x, y, t) = \frac{m}{2\pi i\hbar t}\int_{-a/2}^{a/2} dy' \int_{-a/2}^{a/2} dx' \psi_{\tilde{m},\tilde{n}}(x', y') \times \exp\left\{\frac{im}{2\hbar}\frac{[(x - x')^2 + (y - y')^2]}{t}\right\}. \quad (2)$$

Substituting Eq. (1) into (2), after some algebra, the wave function $\psi_{\tilde{m},\tilde{n}}(x, y, t)$ is given by

$$\psi_{\tilde{m},\tilde{n}}(x, y, t) = \frac{e^{-(i/\hbar)E_{\tilde{m},\tilde{n}}t}}{4i^3 a}[G(x, t; k_{\tilde{m}}, a) - G(x, t; -k_{\tilde{m}}, a)] \times [G(y, t; k_{\tilde{n}}, a) - G(y, t; -k_{\tilde{n}}, a)], \quad (3)$$

with

$$G(x, t; k_{\tilde{m}}, a) = e^{ik_{\tilde{m}}(x+a/2)}[F(\xi(x - a/2, t; k_{\tilde{m}})) - F(\xi(x + a/2, t; k_{\tilde{m}}))], \quad (4)$$

where $E_{\tilde{m},\tilde{n}} = \hbar^2(k_{\tilde{m}}^2 + k_{\tilde{n}}^2)(2m)$, $F(\xi)$ is the complex Fresnel integral, $F(\xi) = \int_0^{\xi} \exp(i\pi u^2/2)du$, and the integral's argument is given by $\xi(x, t; k) = \sqrt{m(\pi\hbar t)}[(\hbar k t/m) - x]$. Figures 1(a)–1(f) depict the numerical results calculated with Eq. (3) and the parameters of $(\tilde{m}, \tilde{n}) = (25, 25)$ to illustrate the wave patterns $|\psi_{\tilde{m},\tilde{n}}(x, y, t)|^2$ at $t = 0, 0.1T$,

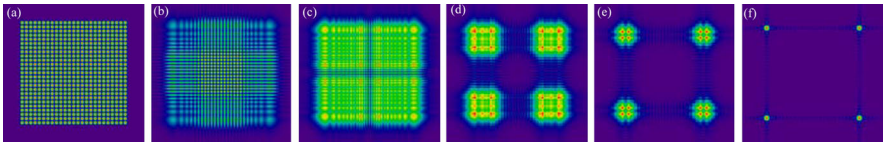

FIG. 1 (color online). Numerical patterns calculated with Eq. (3) and the parameters of $(\tilde{m}, \tilde{n}) = (25, 25)$ to illustrate the wave patterns $|\psi_{\tilde{m},\tilde{n}}(x, y, t)|^2$ at (a) $t = 0$, (b) $0.1T$, (c) $0.25T$, (d) $0.50T$, (e) $1.0T$, and (f) ∞, where T is defined in the text.

$0.25T$, $0.50T$, $1.0T$, and ∞, where $T = 2ma/\hbar k_{\tilde{m}}$ corresponds to the round trip time of the wave in the x direction. The time-evolution wave distributions clearly exhibit strong interference patterns in the time interval between $0.1T$ and T. Note that the wave function $\psi_{\tilde{m},\tilde{n}}(x, y, t)$ in an infinite time is just the Fourier transform of the initial wave function $\psi_{\tilde{m},\tilde{n}}(x, y)$, corresponding to the momentum-space representation. Therefore, the four-lobed beam pattern in Fig. 1(f) reveals the momentum distribution.

The results of recent studies of open square quantum dots show that the wave functions localized on classical periodic orbits are not only the persistent states but also are associated with the striking phenomena of conductance fluctuations [14–16]. The primitive periodic orbits in a 2D square billiard can be described with three parameters (p, q, ϕ), where p and q are two positive integers describing the number of collisions with the horizontal and vertical walls, and the phase factor ϕ is in the range of $-\pi$ to π that is related to the wall positions of specular reflection points [19]. Recently, we have employed the representation of SU(2) coherent states to analytically establish the relation between the quantum wave functions and the classical periodic orbits. As in the Schwinger SU(2) representation, the wave functions associated with periodic orbits (p, q, ϕ) is analytically expressed as $\Psi_{N,M}^{p,q,\phi}(x, y) = \sum_{K=-M}^{M} C_{M,K} e^{iK\phi} \psi_{qN+pK,pN-qK}(x, y)$, where N represents the order of the coherent state and

$$C_{M,K} = 2^{-M}\left[\frac{2M!}{(M-K)!(M+K)!}\right]^{1/2}$$

is the weighting coefficient. Note that the discussion for the asymptotic property of the coherent states can be found in Ref. [19].

The free time evolution of the coherent states $\Psi_{N,M}^{p,q,\phi}(x, y)$ suddenly released at time $t = 0$ can be expressed as $\Psi_{N,M}^{p,q,\phi}(x, y, t) = \sum_{K=-M}^{M} C_{M,K} e^{iK\phi} \times \psi_{qN+pK,pN-qK}(x, y, t)$. Note that the coherent states $\Psi_{N,M}^{p,q,\phi}(x, y)$ behave as the traveling waves in the transverse plane. The standing-wave representation is given by $S_{N,M}^{p,q,\pm\phi}(x, y) = [\Psi_{N,M}^{p,q,\phi}(x, y) \pm \Psi_{N,M}^{p,q,-\phi}(x, y)]/\sqrt{2}$. As a result, the time evolution of the coherent states $S_{N,M}^{p,q,\pm\phi}(x, y)$ suddenly released at time $t = 0$ can be expressed as $S_{N,M,\pm}^{p,q,\phi}(x, y, t) = [\Psi_{N,M}^{p,q,\phi}(x, y, t) \pm \Psi_{N,M}^{p,q,-\phi}(x, y, t)]/\sqrt{2}$. Figures 2(a)–2(f) illustrate the numerical patterns for the wave patterns $|S_{N,M,+}^{p,q,\phi}(x, y, t)|^2$ with the parameters of $(p, q) = (1, 1)$, $(N, M) = (42, 6)$, and $\phi = 0.6\pi$ at $t = 0$, $0.08T$, $0.15T$, $0.25T$, $0.5T$, and ∞, where $T = 2ma/\hbar k_N$ corresponds to the round trip time of the periodic orbit and $k_N = N\pi/a$. It can be seen that the transient dynamics of the coherent state displays not only the feature of classical flow but also the salient interference patterns.

Similarities between paraxial optics and nonrelativistic quantum mechanics have long been recognized and recently been used to make analog studies of quantum wave functions [20]. This correlation has been used to manifest the spatial morphology of wave functions [21] and energy-level statistics [22] in 2D quantum billiards with the oxide-confined vertical-cavity surface-emitting lasers (VCSELs). The literatures [23] revealed that the chessboardlike patterns of the eigenstates $\psi_{\tilde{m},\tilde{n}}(x, y)$ could be similarly generated with the lasing modes from phase-coupled VCSEL arrays or photonic resonator crystals. In addition to resonant stationary states, the free time evolution of quantum wave functions can be expressed as an analogous way to the free-space propagation of coherent lights. However, the free-space propagation of the lasing modes had not been investigated. Here we use the coherent lasing modes generated from the large-aperture VCSELs to experimentally investigate the time evolution of the coherent state.

Schematics of the laser device structure and the experimental setup are shown in Fig. 3. The separability of the wave function in the VCSEL device enables the wave vectors to be decomposed into k_z and k_t, where k_z is the wave-vector component along the direction of vertical emission and k_t is the transverse wave-vector component. Under the circumstance of paraxial optics, $k_t \ll k_z$, the longitudinal field is significantly small in comparison with the transverse field. Therefore, the electric field can be

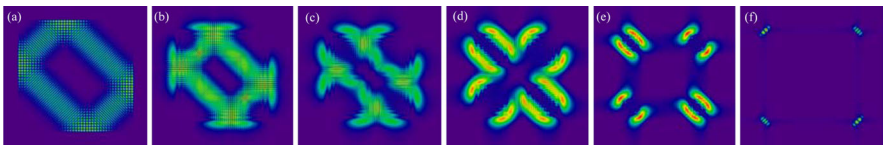

FIG. 2 (color online). Numerical patterns for the wave patterns $|S_{N,M,+}^{p,q,\phi}(x, y, t)|^2$ with the parameters of $(p, q) = (1, 1)$, $(N, M) = (42, 6)$, and $\phi = 0.6\pi$ at (a) $t = 0$, (b) $0.08T$, (c) $0.15T$, (d) $0.25T$, (e) $0.5T$, and (f) ∞, where T is defined in the text.

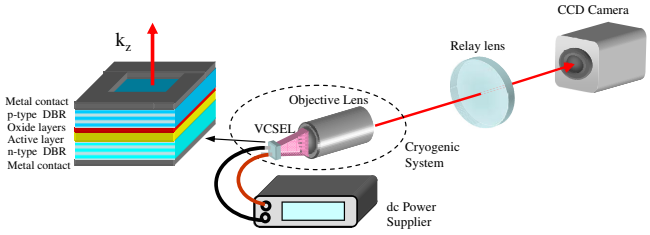

FIG. 3 (color online). Schematics of the laser device structure and the experimental setup. (DBR is distributed Bragg reflector.)

approximated to have only transverse components and no longitudinal component, i.e., so-called quasi-TEM waves. After separating the z component in the wave equation, we are left with a two-dimensional Helmholtz equation: $(\nabla_t^2 + k_t^2)\psi(x, y) = 0$, where ∇_t^2 means the Laplacian operator operating on the coordinates in the transverse plane and $\psi(x, y)$ is a scalar wave function that describes the transverse distribution of the laser mode. Consequently, the transverse modes of the oxide-confined VCSEL device are equivalent to the eigenfunctions of the 2D Schrödinger equation with hard wall boundaries of the same geometry. The vertical cavity is formed by two distributed Bragg reflectors and its optical length is designed to be nearly one wavelength. The resonant optical wave emitted from the cavity end $z = 0$ to the environment in the direction of the $+z$ axis can be expressed as the Fresnel transformation:

$$\psi(x, y, z) = \frac{ie^{-ikz}}{\lambda z} \int dy' \int dx' \exp\left\{-\frac{ik}{2} \times \frac{[(x - x')^2 + (y - y')^2]}{z}\right\} \psi(x', y'). \quad (5)$$

Comparing Eqs. (2) and (5) it is evident that the time evolution of a 2D quantum state is equivalent to the Fresnel transformation of a near-field optical wave with the substitution of $t \rightarrow z$ and $m/\hbar \rightarrow 2\pi/\lambda$, where λ is the lasing wavelength.

First we used square-shaped VCSELs with 40 μm oxide aperture to explore the free-space propagation of coherent modes. The VCSEL devices were placed in a cryogenic system with a temperature stability of 0.1 K at the range of 80–300 K. A current source with a precision of 0.01 mA was utilized to drive the VCSEL device. The transverse patterns at different propagation distances were reimaged onto a CCD camera with a very large numerical aperture (NA) microscope objective lens (Mitsutoyo, NA = 0.9) mounted on a translation stage.

Although an ideal 2D square billiard has many possible eigenstates, the coherent states related to classical periodic orbits with $(p, q) = (1, 1)$ are experimentally found to be the persistent states at the temperature below 260 K. Figure 4(a) shows the near-field pattern of the lasing mode at $T = 260$ K. The experimental transverse patterns for the free-space propagation are shown in Figs. 4(b)–4(e) measured at the positions of $z/z_d = 0.08$, 0.2, 0.35, and 0.70, respectively, where $z_d = 2ak_z/nk_t$ is the characteristic length and n is the refractive index of the semiconductor cavity. Note that the characteristic length of the optical diffraction is analogous to the characteristic time T of the quantum diffraction in time. With the properties that $k_z = 26.3\ \mu\text{m}^{-1}$, $a = 40\ \mu\text{m}^{-1}$, $n = 3.5$, and $k_t = 4.2\ \mu\text{m}^{-1}$, z_d can be found to be approximately 143 μm. Figure 4(f) depicts the far-field pattern which was measured by a digital camera for the direct projection of the laser beam on a paper screen at a distance of ~20 cm from the laser device. It can be seen that the experimental patterns agree quite well with the numerical results shown in Fig. 2. The good agreement validates the fact that the free-space propagation of coherent modes emitted from VCSELs can be employed as an analogous observation of the time evolution of quantum-billiard wave functions.

Next we exploit a deformed-square-shaped VCSEL with a ripple boundary to experimentally study the transient dynamics of the wave functions released from 2D chaotic billiard systems. With a ripple boundary, the experimental near-field patterns are found to be randomly distributed over the laser cavity, i.e., so-called chaotic wave modes. Note that rough billiards and related systems are also of considerable interest elsewhere [24]. Figures 5(a)–5(e) depict the experimental transverse patterns obtained at the near-field position and $z/z_d = 0.25$, 0.4, and 0.6, and the far-field regime, respectively. It can be seen that the transverse patterns in the propagation position between $0.1z_d$ and $1.0z_d$ display a striking feature of random branching behavior with the appearance of intricate interference fringes.

It has been shown that the universal features of stationary chaotic wave functions in quantum billiards can be manifested with a superposition of plane waves of fixed wave-vector magnitude with random amplitude, phase, and direction [25]. Therefore, the standing-wave chaotic wave functions in a deformed square-shaped quantum billiard

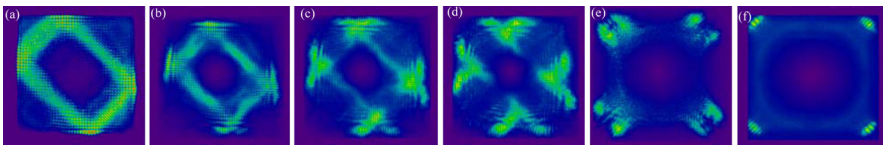

FIG. 4 (color online). Experimental transverse patterns for the free-space propagation of the coherent lasing mode measured at the positions of (a) near field, (b) $z/z_d = 0.08$, (c) $z/z_d = 0.2$, (d) $z/z_d = 0.35$, (e) $z/z_d = 0.70$, (f) far field, where z_d is defined in the text.

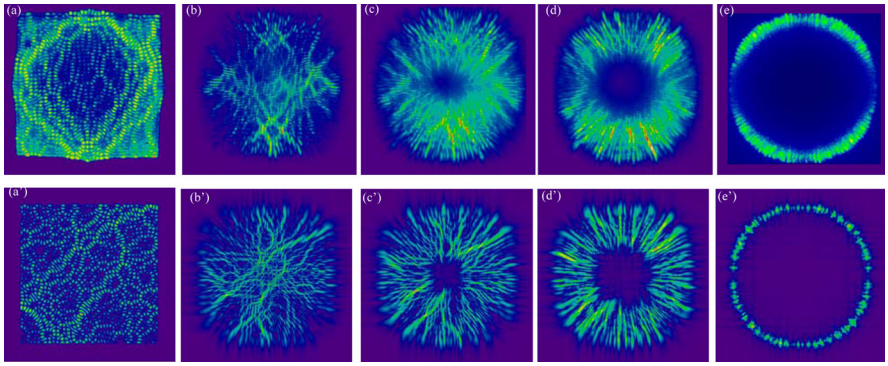

FIG. 5 (color online). Experimental transverse patterns for the free-space propagation of the chaotic mode measured at the positions of (a) near field, (b) $z/z_d = 0.25$, (c) $z/z_d = 0.4$, (d) $z/z_d = 0.6$, (e) far field, where z_d is defined in the text. (a′)–(e′) Numerical patterns calculated with $\Psi(x, y, t) = \sum_{\tilde{m},\tilde{n}} \cos(\phi_{\tilde{m},\tilde{n}}) \psi_{\tilde{m},\tilde{n}}(x, y, t)$ for the time at $t = 0$, $0.25T$, $0.4T$, $0.6T$, and ∞, respectively, where $49^2 < \tilde{m}^2 + \tilde{n}^2 < 51^2$ and $\phi_{\tilde{m},\tilde{n}}$ are random values.

can be described as $\Psi(x, y) = \sum_{\tilde{m},\tilde{n}} \cos(\phi_{\tilde{m},\tilde{n}}) \psi_{\tilde{m},\tilde{n}}(x, y)$, where the eigenstates $\psi_{\tilde{m},\tilde{n}}(x, y)$ in the summation are subject to the condition that the values $\sqrt{k_{\tilde{m}}^2 + k_{\tilde{n}}^2}$ are nearly constant and the phase factors $\phi_{\tilde{m},\tilde{n}}$ are random. With the superposition principle, the free time evolution of the chaotic wave $\Psi(x, y)$ is then given by $\Psi(x, y, t) = \sum_{\tilde{m},\tilde{n}} \cos(\phi_{\tilde{m},\tilde{n}}) \psi_{\tilde{m},\tilde{n}}(x, y, t)$. We use this expression for the states $\psi_{\tilde{m},\tilde{n}}(x, y, t)$ in the range of $49^2 < \tilde{m}^2 + \tilde{n}^2 < 51^2$ and random values for $\phi_{\tilde{m},\tilde{n}}$ to numerically generate typical wave patterns which are shown in Figs. 5(a′)–5(e′) at $t = 0$, $0.25T$, $0.4T$, and ∞. The general features of the numerical patterns are clearly similar to the experimental observation shown in Figs. 5(a)–5(e). Therefore, the free-space propagation of the chaotic modes emitted from VCSELs can be used to manifest the transient dynamics of the chaotic wave functions in quantum billiards.

In conclusion, we have analytically and numerically investigated the diffraction-in-time effect of the eigenstates and coherent states suddenly released from a square quantum billiard. We have utilized the large-aperture VCSEL devices to experimentally verify that the transient dynamics of quantum-billiard wave functions can be analogously observed with the free-space propagation of the coherent lasing modes. Moreover, we have exploited a chaotically shaped laser cavity to originally study the diffraction-in-time characteristics of the chaotic wave functions. The transient wave patterns of chaotic modes are found to display a striking feature of random branching interference fringes. We believe that the present investigation can provide an important insight into quantum physics and wave optics.

This work is supported by the National Science Council of Taiwan (Contract No. NSC-97-2112-M-009-016-MY3).

*yfchen@cc.nctu.edu.tw

[1] M. Moshinsky, Phys. Rev. **88**, 625 (1952).
[2] S. Godoy, Phys. Rev. A **65**, 042111 (2002); M. Kleber, Phys. Rep. **236**, 331 (1994).
[3] E. Granot and A. Marchewka, Europhys. Lett. **72**, 341 (2005).
[4] V. I. Man'ko, M. Moshinsky, and A. Sharma, Phys. Rev. A **59**, 1809 (1999).
[5] A. del Campo, J. G. Muga, and M. Moshinsky, J. Phys. B **40**, 975 (2007).
[6] G. G. Paulus, F. Lindner, H. Walther, A. Baltuška, E. Goulielmakis, M. Lezius, and F. Krausz, Phys. Rev. Lett. **91**, 253004 (2003).
[7] C. E. Wieman, D. E. Pritchard, and D. J. Wineland, Rev. Mod. Phys. **71**, S253 (1999), and references therein.
[8] T. Hils, J. Felber, R. Gähler, W. Gläser, R. Golub, K. Habicht, and P. Wille, Phys. Rev. A **58**, 4784 (1998).
[9] A. Steane, P. Szriftgiser, P. Desbiolles, and J. Dalibard, Phys. Rev. Lett. **74**, 4972 (1995).
[10] F. Lindner, M. G. Schätzel, H. Walther, A. Baltuška, E. Goulielmakis, F. Krausz, D. B. Milošević, D. Bauer, W. Becker, and G. G. Paulus, Phys. Rev. Lett. **95**, 040401 (2005).
[11] Y. Colombe, B. Mercier, H. Perrin, and V. Lorent, Phys. Rev. A **72**, 061601 (2005).
[12] F. Delgado, H. Cruz, and J. G. Muga, J. Phys. A **35**, 10 377 (2002).
[13] F. Delgado, J. G. Muga, D. G. Austing, and G. García-Calderón, J. Appl. Phys. **97**, 013705 (2005).
[14] R. Akis and D. K. Ferry, Phys. Rev. B **59**, 7529 (1999).
[15] I. V. Zozoulenko and K. F. Berggren, Phys. Rev. B **56**, 6931 (1997).
[16] J. P. Bird, R. Akis, D. K. Ferry, D. Vasikska, J. Cooper, Y. Aoyagi, and T. Sugano, Phys. Rev. Lett. **82**, 4691 (1999).
[17] A. del Campo, I. Lizuain, M. Pons, J. G. Muga, and M. Moshinsky, J. Phys. Conf. Ser. **99**, 012003 (2008).
[18] J. Wiersig, Phys. Rev. E **64**, 026212 (2001).
[19] Y. F. Chen, K. F. Huang, and Y. P. Lan, Phys. Rev. E **66**, 046215 (2002).
[20] D. Dragoman and M. Dragoman, *Quantum-Classical Analogies* (Springer-Verlag, Berlin, 2004), and references cited therein.
[21] K. F. Huang, Y. F. Chen, H. C. Lai, and Y. P. Lan, Phys. Rev. Lett. **89**, 224102 (2002); C. C. Chen, C. C. Liu, K. W. Su, T. H. Lu, Y. F. Chen, and K. F. Huang, Phys. Rev. E **75**, 046202 (2007).
[22] T. Gensty, K. Becker, I. Fischer, W. Elsäßer, C. Degen, P. Debernardi, and G. P. Bava, Phys. Rev. Lett. **94**, 233901 (2005).
[23] H. Pier, E. Kapon, and M. Moser, Nature (London) **407**, 880 (2000).
[24] Y. Hlushchuk, L. Sirko, U. Kuhl, M. Barth, and H. J. Stöckmann, Phys. Rev. E **63**, 046208 (2001); N. Savytskyy, O. Hul, and L. Sirko, *ibid.***70**, 056209 (2004).
[25] M. V. Berry, J. Phys. A **10**, 2083 (1977); P. O'Connor, J. Gehlen, and E. J. Heller, Phys. Rev. Lett. **58**, 1296 (1987).